SiliconPV 2025, 15th International Conference on Crystalline Silicon Photovoltaics
Characterisation, Modelling and Simulation
https://doi.org/10.52825/siliconpv.v3i.2695

Published: 20 Jan. 2026

Simulation and Analysis of PECVD Process for Silicon Nitride Deposition Using CFD: Impact of Pressure on Deposition Uniformity

Vinay Prasad[1] and Arun Appadurai[1,*]

[1]Adani New Industries Ltd., India

*Correspondence: Arun Appadurai, ArunMangala.PrakashA@adani.com

Abstract. This study presents a computational fluid dynamics (CFD)-based simulation of the plasma-enhanced chemical vapor deposition (PECVD) process utilizing COMSOL Multiphysics. Specifically, the research focuses on the deposition of silicon nitride (SiN_x) on silicon wafers, where this layer functions as an anti-reflective coating (ARC) to enhance light absorption. Regardless of the solar technology in question such as passivated emitter and rear contact (PERC), tunnel oxide passivated contact (TOPCon), hetero-junction technology (HJT), or tandem, understanding the deposition of ARC is crucial. This work simulates the multi-physics involved in PECVD process, encompassing fluid flow, plasma reactions, gas-phase reactions, and surface reactions. In this work we successfully demonstrated the modelling of the complex PECVD process capturing various physics like fluid flow, plasma physics, heavy species transports, and plasma, gas-phase, as well as surface reactions, and further validated it experimentally. The model was then used for various parametric studies i.e., effect of input parameters like pressure and temperature on the key output parameter i.e., deposition rate. This research not only demonstrates the capability of simulating intricate solar manufacturing processes like PECVD but also lays the groundwork for future simulation-based optimization of such processes and creating digital-twins as a part of Industry 4.0. This study represents the first documented investigation in the literature to report electron density distribution and transient thin film growth dynamics on silicon wafers within a tubular PECVD chamber.

Keywords: PECVD, SiNx Deposition, CFD Simulation, COMSOL, Anti Reflective Coating

1. Introduction

Plasma-enhanced chemical vapor deposition (PECVD) has become a cornerstone in the field of thin-film deposition, particularly within the photovoltaic (PV) manufacturing industry. This process, which transitions materials from a gaseous state to a solid state on a substrate, is facilitated by gas-phase chemical reactions occurring within a plasma of the reacting gases. The process begins with the generation of plasma, typically achieved through radio frequency (RF), alternating current (AC), or direct current (DC) discharge between two electrodes. The space between the electrodes is filled with reacting gases. In this plasma state, a significant percentage of the gas atoms or molecules become ionized. The degree of ionization can range from low density plasma in typical capacitive discharges to high-density plasma in inductive discharges. Energetic electrons within the plasma induce many processes that are otherwise improbable at low temperatures, such as dissociation of precursor molecules and the creation of free radicals. These reactions lead to the deposition of thin films on the substrate. Surfaces exposed to plasma undergo energetic-ion bombardment which enhances film density and re-

moves contaminants, thereby improving the film's electrical and mechanical properties. However, this direct ion bombardment can also introduce surface-defects, which are a known drawback of plasma exposure. The primary advantages of PECVD over conventional CVD are lower deposition temperatures, stronger mechanical strength due to lower thermal stress, good conformity and step coverage on uneven surfaces, tighter control of the thin film process, and high deposition rates. The above advantages outweigh risks and make PECVD a crucial process in solar manufacturing for deposition of various layers like amorphous silicon, anti-reflective/passivating coatings like silicon nitride/silicon oxy-nitride and aluminium oxide.

2. Literature Review

This section delves into the research on numerical modelling of PECVD processes. Collins and White [1] developed a CFD model using FLUENT for the PECVD of silicon nitride. The finalized reactions include three plasma reactions, two gas phase chemical reactions, and four surface reactions. Among the investigated parameters like N_2 flow, SiH_4/NH_3 (ratio), SiH_4+NH_3, pressure, RF/gap (power density), and the electrode gap, the sum of SiH_4 and NH_3 was identified as having the most significant impact on the deposition rate. Cao et at. [2] developed a verified multi-physics simulation model using COMSOL to analyze silicon nitride film deposition via in-line PECVD, a key process in solar cell manufacturing. It highlights how optimizing both structural and process parameters such as microwave tube placement, gas flow, and temperature can significantly enhance film thickness and deposition rate, offering practical insights for industrial PECVD system design. Xia et al. [3] presented a comprehensive multi-physics simulation of silicon nitride thin-film deposition in a 300 mm PECVD reactor, integrating plasma dynamics, chemical reactions, and fluid flow. After validating the model with full-wafer experimental data, they demonstrated how reactor design, especially showerhead configuration, significantly influences deposition uniformity and film composition. Wan et al. [4] explored how PECVD process parameters affect the structural and electronic properties of SiN_x films used in solar cells. They optimized film conditions that enable both high optical transmission and effective surface passivation, overcoming the typical trade-off between these two qualities. Silva and Morimoto [5] conducted a two-dimensional gas flow simulation of an in-house PECVD-TEOS reactor, primarily used for deposition of silicon oxide layer on the substrate using tetraethyl orthosilicate (TEOS) as precursor. Utilizing the FLOTRAN-CFC code within the ANSYS simulator, they predicted the velocity and temperature profiles within the reactor. The study aimed to optimize the gas flow system by examining the behavior of the gas flow through the PECVD reactor. The findings showed considerable influence of the reactor geometry and deposition process pressure on the velocity distribution curves. Further the study concluded that reactor geometry affects gas flow behavior and modifying the gas flow entrance alters the gas velocity profile, independent of process pressure. The research highlights better gas flow distribution without any recirculation zone as a crucial factor to better quality and uniform thin-film deposition. For example, low gas velocity due to a large distance between electrodes can result in longer residence time for the gases. This increased residence time promotes vapor phase reactions during the deposition, causing the film to deposit on the reactor walls rather than uniformly on the substrate. Consequently, the deposited thin film may have a nonuniform thickness, poor structural properties, and inconsistent composition, which are indicators of low quality in thin film deposition processes. Crose et al. [6] presented a multiscale CFD simulation framework in ANSYS software, including both a macroscopic CFD model and a microscopic surface interaction kinetic Monte-Carlo model. This framework was applied to a-Si:H thin film deposition via PECVD. The study underscores the critical role of multiscale models in predicting and improving PECVD reactor geometries and operating conditions. The PECVD reactor simulated in this research belongs to the widely used subclass of CVD reactors known as chambered parallel-plate reactors. The study accounts for twelve dominant species and thirty-four gas phase reactions that lead to film growth. The authors emphasize the necessity of such detailed modelling for improving reactor geometries and flow characteristics in PECVD process. Later, Crose et al. [7] extended their PECVD numerical model to optimize the deposition of amorphous silicon on silicon substrates with a three-dimensional

PECVD reactor. By applying the model to two representative PECVD reactor geometries, they demonstrated that thickness non-uniformity in the a-Si:H product can be minimized by adjusting the positions and size of the showerhead holes. The 3D CFD model not only promises improvements in product quality for PECVD processing but also offers significant savings in time and resources otherwise spent on physical testing and manufacturing. Lee et al. [8] conducted experimental and numerical studies on the deposition of amorphous carbon layers (ACL) on wafers using a showerhead based PECVD reactor composed of two stages of porous media. The study concluded that ACL growth could be optimized by controlling the fluid velocity gradient in the shower head. This was achieved through modification of the hole density in the perforated plate. Zhou et al. [9] developed a coupled multi-physics field model using the COMSOL Multiphysics platform to simulate the deposition of SiN_x:H thin films via low-frequency PECVD (LF-PECVD). The deposition process was simulated through a coupled analysis of the fluid flow, heat transfer, chemical reactions, and plasma reactions. Dominant reactions were identified as nine plasma reactions, seventeen gas-phase reactions, and nine surface chemical reactions. The study investigated the effects of temperature, pressure, total flow rate, and SiH_4/NH_3 flow ratio on the deposition rate and uniformity of the deposited SiN_x:H films.

3. Problem Definition

3.1 Two-Wafer Model: Part 1

The wafer level deposition process is simulated using a two-dimensional model. The computational domain is depicted in Fig. 1. The domain encompasses the region between two adjacent wafers filled with precursor gases SiH_4 and NH_3 and is modelled as a fluid. Importantly, flow of fluid is neglected due to the minimal fluid movement in the domain. The problem is diffusion-dominant in the plane of interest. The simulation employs a low frequency (40 kHz) PECVD process, with reactions referenced from Cao et al. [2].

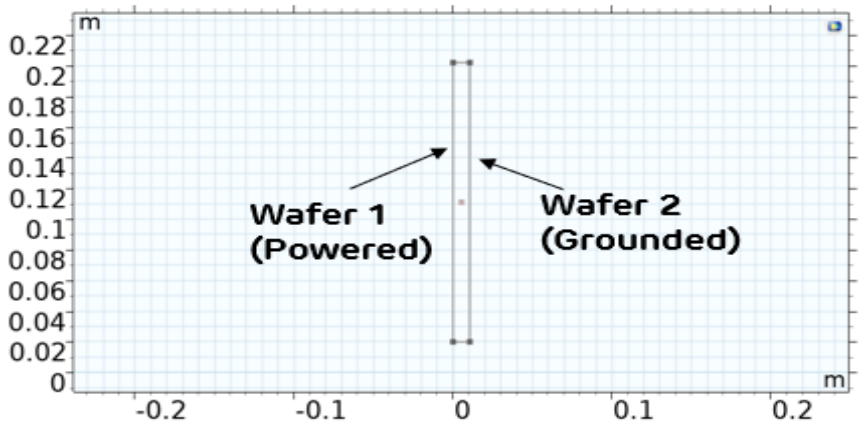

Figure 1. *Computational geometry for two-wafer model.*

3.1.1 Computational Mesh

A structured mesh, depicted in Fig. 2, is used for the discretization of the computational domain. The mesh elements close to the surface are more densely packed to ensure proper resolution of the surface reactions responsible for the silicon nitride deposition. A grid independence study was conducted to ensure adequate resolution.

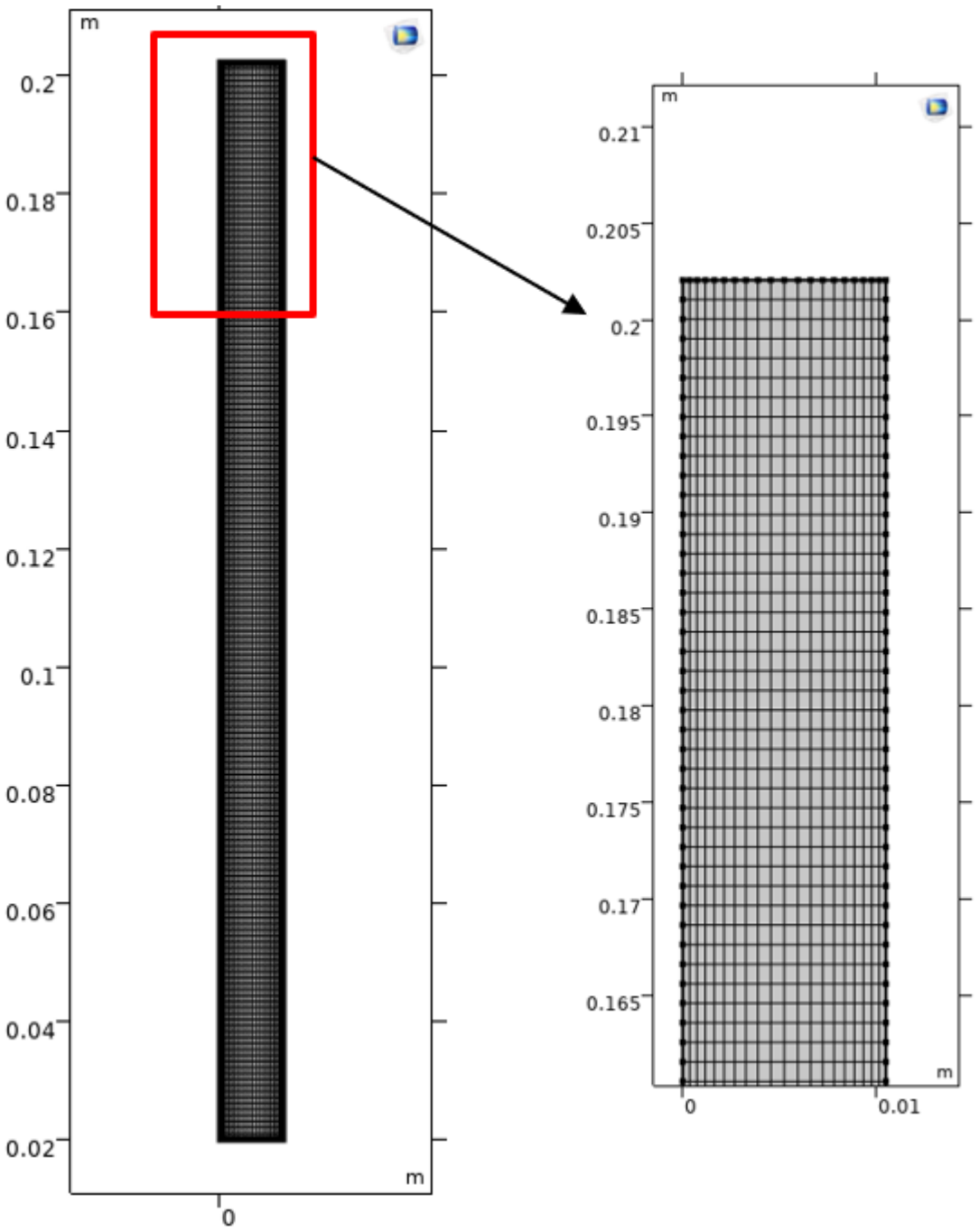

Figure 2. *Computational mesh for 2-wafer model.*

3.2 Complete Tube Model: Part 2

The spatial distribution and uniformity are studied using a two-dimensional model of the PECVD tube. The computational domain is two dimensional, comprising a fluid domain that encloses the plasma domain (indicated in blue) as shown in Fig. 3. For simplicity in modelling, the electrodes within the plasma domain function as a slip wall for the fluid. The fluid flow is one-way coupled with the plasma domain. These assumptions are acceptable as the primary objective of this study is to qualitatively understand the influence of pressure on the uniformity of deposition along the boat.

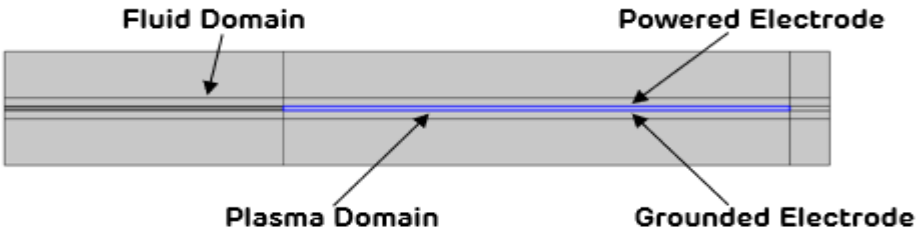

Figure 3. *Computational geometry for complete tube model.*

3.2.1 Computational Mesh

A fully structured mesh, illustrated in Fig. 4, with an average element quality of 1.0 is used for the discretization of the computational domain. The mesh elements are more densely packed closer to the tube walls. Further, finer grid resolution is employed within the plasma domain, highlighted as blue rectangle in Fig. 3, A grid independence study was conducted once again to ensure adequate resolution.

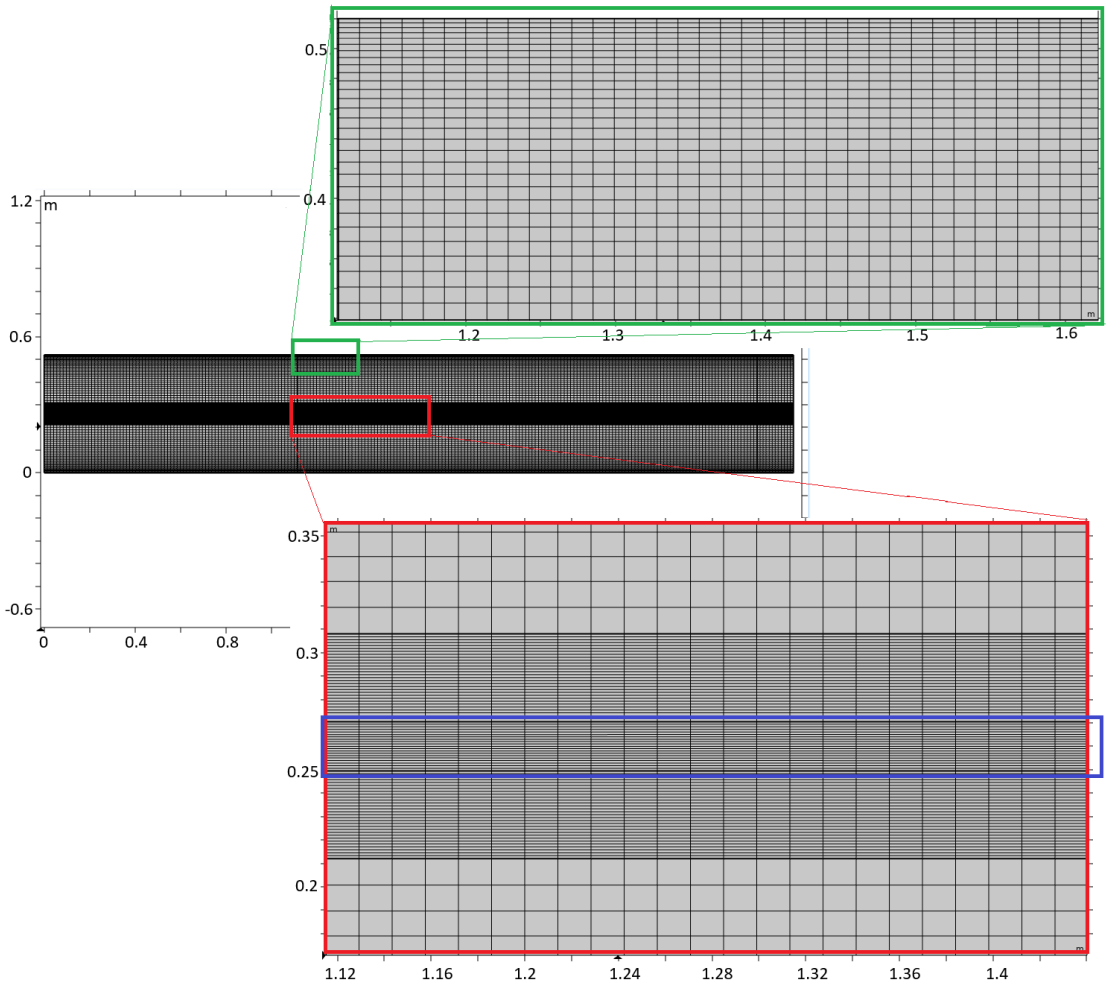

Figure 4. *Computational mesh for complete tube model.*

4. Governing Equations

An overview of the governing equations involved in the PECVD process is provided in this section. The model geometry is developed and the necesary grid generated based on the

geometry. The domain is further setup with initial and boundary conditions whose details are given in Table 1. In the table, $|\boldsymbol{v}|$ represents velocity magnitude, P is the pressure, u_{inlet} is the magnitude of inlet velocity, P_{outlet} is the outlet pressure, n_e is the electron density, V_0 is the plasma voltage amplitude, f is the plasma power frequency, and t is the instantenous time. The necessary physics are explained below. The models are numerically solved using COMSOL Multiphysics software version 6.2 in a 24-core Dell worskstation. The detailed mathematical formulation can be found in [1-3].

Table 1. *Initial and Boundary conditions used in the present study. Here, FD, PD, TW, and CT denote Fluid Domain, Plasma Domain, Two-Wafer model, and Complete-Tube model, respectively.*

FD	TW	Diffusion Model	-
FD	CT	Initial Condition	$\|\boldsymbol{v}\|$ = 0 m/s, P = 0 Pa
FD	CT	Inlet Boundary	u_{inlet} = 5.526 m/s
FD	CT	Outlet Boundary	P_{outlet} = 0 Pa
FD	CT	Walls	No-Slip
PD	TW/CT	Initial Condition	$n_e = 10^{14}$ m^{-3}
PD	TW/CT	Metal Electrode	$V_0 \sin(2\pi ft)$ V
PD	TW/CT	Grounded	0 V
PD	TW/CT	Walls	De-ionization

4.1 Mass Conservation

Conservation of mass is ensured by

$$\frac{\partial \rho}{\partial t} + \nabla \cdot (\rho \boldsymbol{v}) = 0 \tag{1}$$

where ρ is the weighted-average density, $\boldsymbol{v}$ is the velocity vector, and t denotes time.

4.2 Momentum Conservation

The conservation of momentum is ensured using the Navier-Stokes equation

$$\frac{\partial (\rho \boldsymbol{v})}{\partial t} + \rho(\boldsymbol{v} \cdot \nabla)\boldsymbol{v} = -\nabla P + \nabla \cdot \boldsymbol{\tau} + S_m \tag{2}$$

where P is the pressure, $\boldsymbol{\tau}$ is the stress tensor, and S_m is the source term.

4.3 Electron Drift-Diffusion

The transport of electron is modelled using the drift-diffusion model

$$\frac{\partial n_e}{\partial t} + \nabla \cdot \boldsymbol{\Gamma}_e = R_e \tag{3}$$

where n_e is the electron density, R_e is electron generation rate based on the ionization reaction, and Γ_e represents total electron flux vector given by:

$$\boldsymbol{\Gamma}_e = -n_e \mu_e \boldsymbol{E} - D_e \nabla n_e \tag{4}$$

where the first term on the right-hand side represents transport of electrons due to electric field $\boldsymbol{E}$ while the second term represents transport due to the concentration gradient. Here μ_e denotes electron mobility while D_e denotes electron diffusion coefficient.

Note that for the electron temperature, the Druyvesteyn model [10] of electron energy distribution function has been used.

4.4 Heavy Species Transport

The PECVD process of silicon nitride deposition involves a wide range of plasma discharge reactions, gas-phase chemical reactions, and surface reactions. The precursors are ionized and dissociated in plasma phase to form highly reactive radicals. The radicals react with each other in gas-phase reactions to form key species like $SiNH_3$, that finally reacts with the wafer surface to form the silicon nitride coating. The list of dominant reactions is given in Fig. 5.

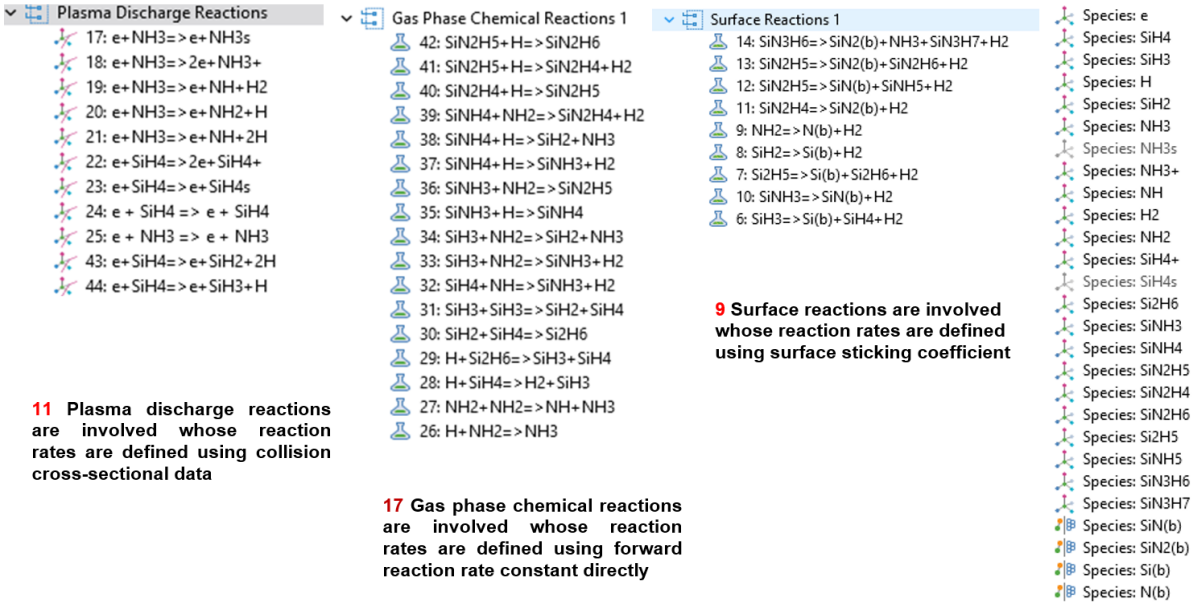

Figure 5. *Snapshot from the COMSOL interface illustrating the list of reactions used.*

The chain of reactions require transport of species from the core of the plasma to the reacting surface, which is governed by

$$\frac{\partial(\rho Y_i)}{\partial t} + \nabla \cdot (\rho \boldsymbol{v} Y_i) = -\nabla \cdot \boldsymbol{J_i} + R_i \tag{5}$$

$$\boldsymbol{J_i} = -\rho D_i \nabla Y_i \tag{6}$$

$$\rho = \frac{P}{RT} \sum x_i M_i \tag{7}$$

where Y_i is the heavy species mass fraction for species i, $\boldsymbol{J_i}$ is the diffusive flux, R_i is the material generation rate, and D_i is the diffusion coefficient.

4.5 Deposition Height

The surface reactions lead to the deposition of the bulk species on the wafer surface.The resulting deposition rate is predicted using the equation given below.

$$\frac{\mathrm{d}H_i}{\mathrm{d}t} = \frac{R_{surf,i} M_i}{\Gamma_{tot}} \tag{8}$$

where H_i is the deposition height for species i, $R_{surf,i}$ is the surface rate expression, M_i is the molar mass, and Γ_{tot} is the total surface site concentration.

5. Validation

The validation of the simulation models was done using two key parameters of deposition i.e., deposition rate and nitrogen to silicon ratio (*N/Si*) which correlates to the refractive index of the deposited layer.

The deposition rate predicted by the 2-wafer simulation model was about 8.8 nm/min. For similar operating conditions, the physical deposition rate measured from the PECVD reactor was approximately 7.4 nm/min. Although the model is primarily designed to simulate deposition on wafer surfaces, it is important to acknowledge that, in practice, material deposition also occurs on the wafer carrier (boat). Thus, the over-prediction in the model could be explained by the loss of precursors due to the deposition in the boat.

Further, the *N/Si* ratio in the simulation model was calculated as it is reported that this ratio correlates well with the refractive index [11]. Under similar operating conditions, the ellipsometry measurement of the deposited layer in the PECVD reactor was conducted and its refractive index was measured to be 2.02. In the simulation model, the equations used for the calculation of the *N/Si* ratio are as follows.

$$c_N = \sum_i \xi_{N,i} v_{film,i} J_i \tag{9}$$

$$c_{Si} = \sum_i \xi_{Si,i} v_{film,i} J_i \tag{10}$$

where $c_{N/Si}$ is the mole generation rate of nitrogen/silicon in the solid film of silicon nitride, $\xi_{N/Si,i}$ is the number of moles of nitrogen/silicon element in the solid component, $v_{film,i}$ is the stoichiometric coefficient of the solid component for the i^{th} surface reaction and J_i is the total diffusive flux for the i^{th} absorbed species. The ratio of nitrogen to silicon can be computed as

$$\frac{N}{Si} = \frac{c_N}{c_{Si}} \tag{11}$$

The simulation model predicts N/Si ratio as 1.0003. This N/Si ratio can be converted to a refractive index (*n*) value based on an empirical relation given by Debieu et al. [11].

$$\frac{N}{Si} = \frac{4}{3} \frac{n_{a-Si} - n}{n + n_{a-Si} - 2n_{a-Si_3N_4}} \tag{12}$$

where the $n_{a\text{-}Si}$ value is 3.3 and the $n_{a\text{-}Si3N4}$ value is 1.85 [11]. Using eq. 12, the refractive index of the layer *n* is calculated to be 2.06 which compares favorably to the actual measured value.

6. Results & Discussions

6.1 Two-Wafer Model (Part 1)

The electron density distribution (Fig. 6) becomes symmetric shortly after the plasma power (40 kHz) is activated, transitioning from an initial concentration near the powered electrode (adjacent to the left wafer) towards the center region. Consequently, although the deposition is almost symmetric, the right wafer lags slightly in deposition height (a difference of 1e-9 nm) from the maximum height achieved for the left wafer (1.93e-7 nm). The deposition rate is predicted for the simulated physical time of 3e-6 s and then extrapolated linearly to arrive at a figure for minutes (8.8 nm/min) as explained in Figure 6 (right). The deposition starts flat, but the rate of deposition increases as the plasma stabilizes at the center.

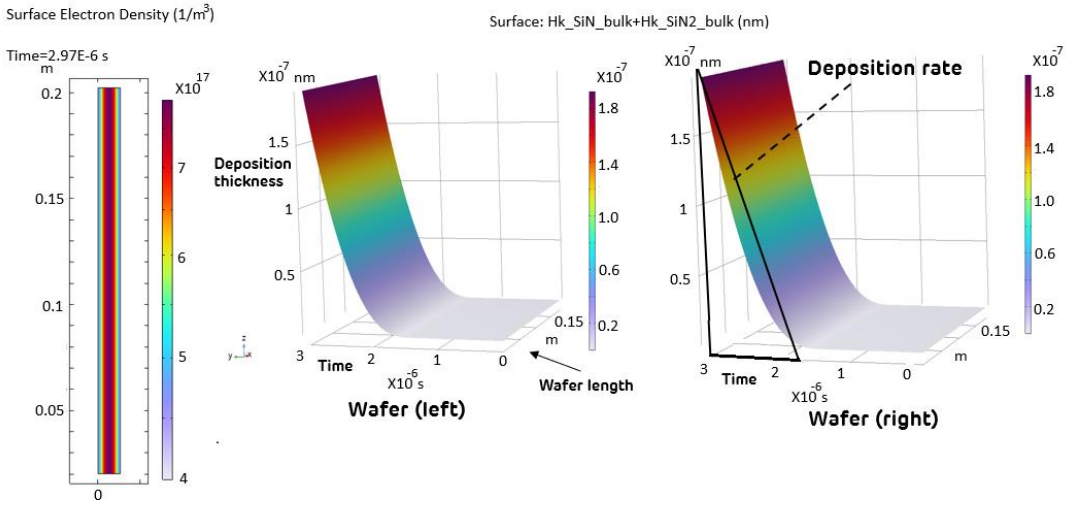

Figure 6. *Electron density distribution and transient deposition of SiN_x.*

6.1.1 Effect of Temperature

Figure 7 shows the inverse relationship of chamber temperature with the silicon nitride deposition rate. For every degree reduction in chamber temperature, the deposition rate increases by approximately 0.06 nm/min. However, reduction in chamber temperature affects other factors including reaction kinetics, film stress, plasma density and more importantly the uniformity of deposition. Similar findings are reported in [12, 5] and the reason for lower deposition rates at elevated temperature is reported to be the densification of the deposited film.

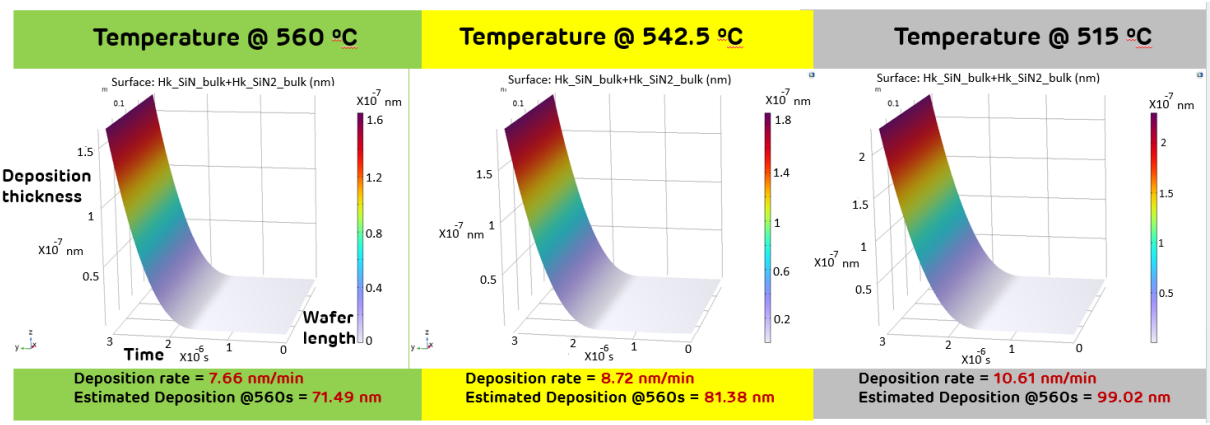

Figure 7. *Effect of temperature on the deposition of silicon nitride.*

6.2 Complete Tube Model (Part 2)

The velocity distribution in Fig. 8 represents the steady state fluid flow in the reactor. This field is frozen and used subsequently for the transient simulation of the plasma domain. The assumption is valid as the fluid reaches a steady state at approximately 5 s which is significantly shorter than the actual PECVD timescale of 500s. Furthermore, as shown in Fig. 9, the velocity field in the plasma domain remains nearly constant across the length of the electrode while the pressure plot exhibits a linear decrease. Therefore, it is anticipated that the uniformity of deposition along the boat will be influenced by pressure.

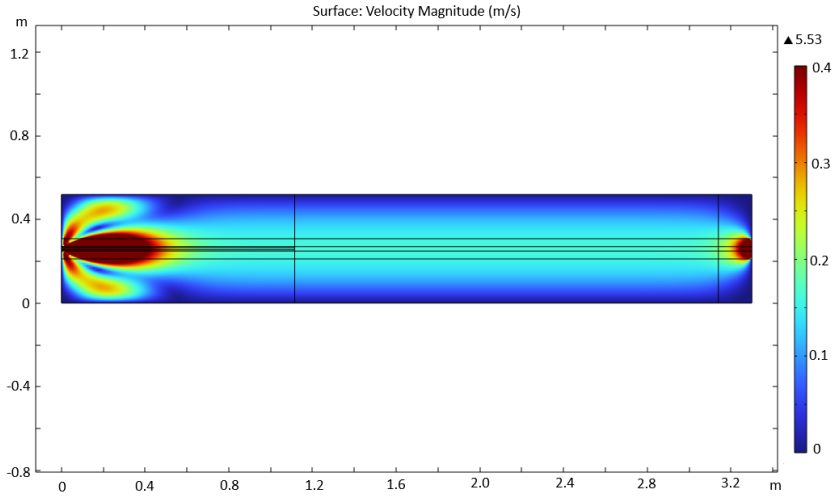

Figure 8. *Velocity field in the PECVD chamber.*

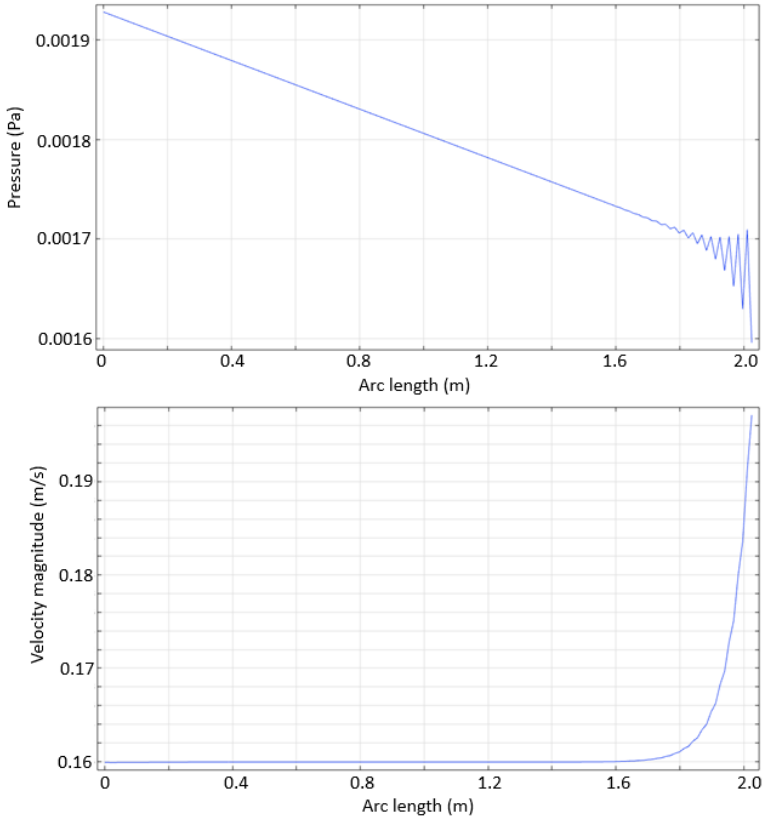

Figure 9. *Pressure (top) and velocity magnitude (bottom) along electrode length (arc length) in the PECVD chamber.*

As shown in Fig. 10, the electron density distribution becomes symmetric shortly after plasma power (40 kHz) is turned on. Although almost symmetric, Fig. 10 shows deposition on the powered electrode lagging by a small insignificant magnitude (insignificant) in deposition height. Also, the deposition starts flat, but the slope increases as the plasma attains its stable symmetric form.

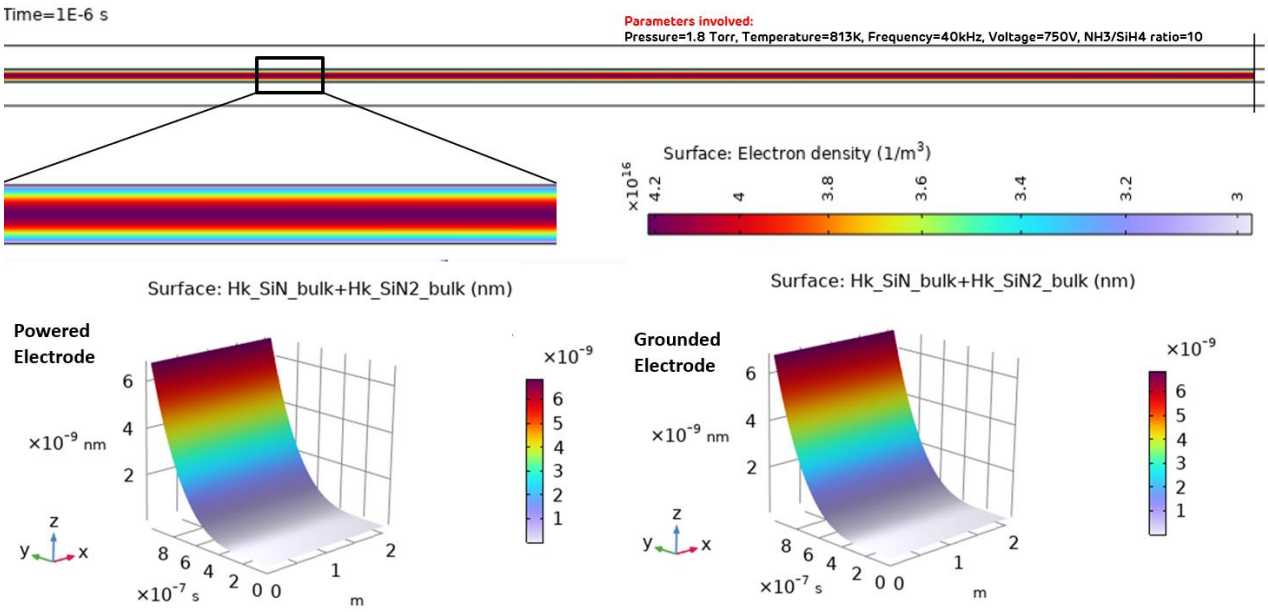

Figure 10. *Electron density distribution and transient deposition of SiN_x.*

Further, for varying chamber pressures, wafer-to-wafer uniformity is calculated using the expression $(Th_{max}+Th_{min})/(2Th_{max})$ where *Th* represents deposition thickness. Figure 11 shows that the decrease in chamber pressure improves the thickness uniformity, suggesting better uniformity at low chamber pressures.

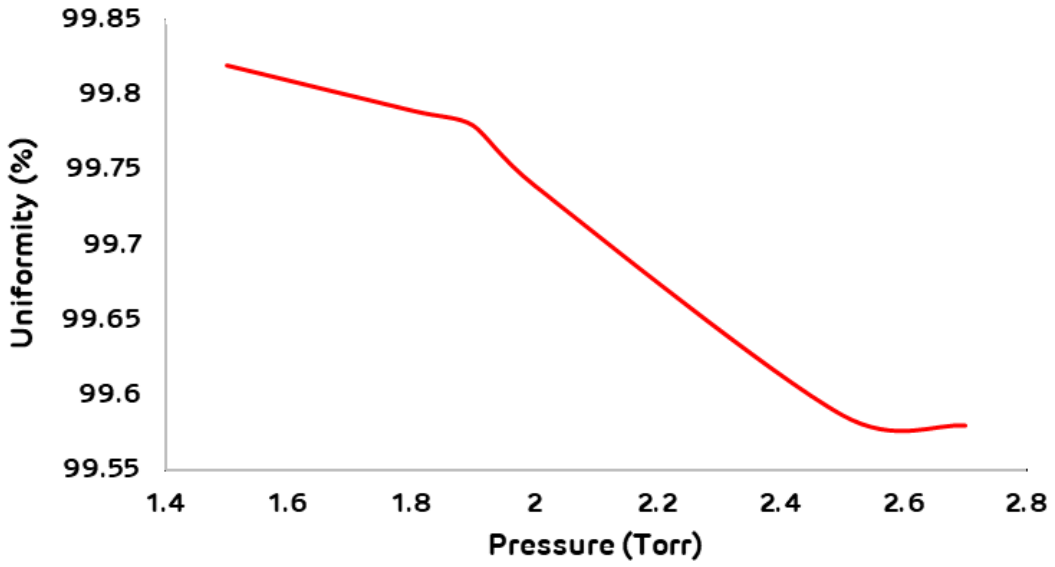

Figure 11. *Variation of wafer-to-wafer uniformity with chamber pressure.*

7. Conclusions

This study demonstrates the use of computational fluid dynamics (CFD) and COMSOL Multiphysics to simulate the plasma-enhanced chemical vapor deposition (PECVD) process, specifically focusing on the key parameters i.e., pressure and temperature affecting the deposition of silicon nitride (SiN_x) on silicon wafers. Key findings include the symmetric electron density distribution achieved shortly after plasma activation, validation of the simulation models with experimental measurements from an operational PV cell manufacturing line and the impact of chamber pressure on wafer-to-wafer deposition uniformity. Overall, this research highlights the

applicability of fluid dynamics, reaction kinetics and other coupled multi-physics methodologies to simulating complex solar manufacturing processes and also sets the stage for future simulation-based optimizations, providing valuable insights into the PECVD process and its parameters.

Data availability statement

The data that support the findings of this study are available from the corresponding author upon reasonable request.

Author contributions

Vinay Prasad: Conceptualization (equal); Data curation (equal); Formal analysis (equal); Investigation; Methodology; Validation; Visualization; Writing-original draft; Writing-review and editing. Arun Appadurai: Conceptualization (equal); Data curation (equal); Formal analysis (equal); Supervision; Project administration; Resources; Writing-review and editing (lead).

Competing interests

The authors declare that they have no competing interests.

References

[1] D.J. Collins, A.J. Strojwas, D.D. White, “A CFD model for the PECVD of silicon nitride” IEEE Trans. Semicond. Manuf., 7 (2) 176-183 (1994) https://doi.org/10.1109/66.286853
[2] Y. Cao, J. Zhou, Y. Ren, W. Xu, W. Liu, X. Cai, B. Zhao, “Study on effect of process and structure parameters on SiNxHy growth by in-line PECVD” Sol. Energy, 198 469-478 (2020) https://doi.org/10.1016/j.solener.2020.01.054
[3] H. Xia, D. Xiang, W. Yang, P. Mou, “Multi-model simulation of 300 mm silicon-nitride thin-film deposition by PECVD and experimental verification” Surf. Coat. Technol., 297 1-10 (2016) https://doi.org/10.1016/j.surfcoat.2016.04.034
[4] Y. Wan, K.R. McIntosh, A.F. Thomson, “Characterisation and optimisation of PECVD SiNx as an antireflection coating and passivation layer for silicon solar cells” AIP Adv., 3 (3) (2013) https://doi.org/10.1063/1.4795108
[5] A.N. Silva, N. Morimoto, “Gas flow simulation in a PECVD reactor” Proc. Int. Conf. Modeling and Simulation of Microsystems – MSM, 434-437 (2002)
[6] M. Crose, A. Tran, P.D. Christofides, “Multiscale computational fluid dynamics: Methodology and application to PECVD of thin film solar cells” Coatings, 7 (2) 22 (2017) https://doi.org/10.3390/coatings7020022
[7] M. Crose, W. Zhang, A. Tran, P.D. Christofides, “Multiscale three-dimensional CFD modeling for PECVD of amorphous silicon thin films” Comput. Chem. Eng., 113 184-195 (2018) https://doi.org/10.1016/j.compchemeng.2018.03.011
[8] G. Lee, D.K. Sohn, S.H. Seok, H.S. Ko, “The effect of hole density variation in the PECVD reactor showerhead on the deposition of amorphous carbon layer” Vacuum, 163 37-44 (2019) https://doi.org/10.1016/j.vacuum.2019.02.009
[9] J. Zhou, J. Huang, J. Liao, Y. Guo, Z. Zhao, H. Liang, “Multi-field simulation and optimization of SiNx:H thin-film deposition by large-size tubular LF-PECVD” Sol. Energy, 228 575-585 (2021) https://doi.org/10.1016/j.solener.2021.09.075
[10] R.J. Carman, R.P. Mildren, “Electron energy distribution functions for modelling the plasma kinetics in dielectric barrier discharges” J. Phys. D: Appl. Phys., 33 (19) L99 (2000) https://doi.org/10.1088/0022-3727/33/19/101

[11] O. Debieu, R.P. Nalini, J. Cardin, X. Portier, J. Perrière, F. Gourbilleau, “Structural and optical characterization of pure Si-rich nitride thin films” Nanoscale Res. Lett., 8 31 (2013) https://doi.org/10.1186/1556-276X-8-31

[12] Berkeley Nanolab, “PECVD Process Manual” (n.d.) https://nanolab.berkeley.edu/process_manual/chap6/6.20PECVD.pdf